Modelling of crud growth phenomena on PWR fuel rods under nucleate boiling conditions

Alexandre Ferrer, Frédéric Dacquait, B. J. P. Gall, Gilles Ranchoux, Geoffroy Riot

Modelling of crud growth phenomena on PWR fuel rods under nucleate boiling conditions

※
※

A. Ferrer (CEA, DEN), France, alexandre.ferrer@cea.fr
F. Dacquait (CEA, DEN), France, frederic.dacquait@cea.fr
B. Gall (IPHC/UDS), France, benoit.gall@iphc.cnrs.fr
G. Ranchoux (EDF/SEPTEN), France, gilles.ranchoux@edf.fr
G. Riot (AREVA NP), France, geoffroy.riot@areva.com

※
※

ABSTRACT

PWR primary circuit materials undergo general corrosion leading to a release of metallic element release and subsequent process of particle deposition and ion precipitation on the primary circuit surfaces. The species accumulated on fuel rods are activated by neutron flux. Consequently, crud erosion and dissolution induce primary coolant contamination.
In French PWRs, ^{58}Co volume activity is generally low and almost constant (< 30 MBq.m^{-3}) throughout an ordinary operating cycle. In some specific cases, a significant increase in volume activity is observed after the middle of a cycle (100-1000 MBq.m^{-3} for ^{58}Co) when conditions for nucleate boiling are locally reached in certain fuel assemblies. Indeed, it is well known that nucleate boiling intensifies the deposition process. The thickness of the crud layer can reach some micrometers in non-boiling areas, whereas it can reach 100 micrometers in boiling areas.

Crud growth in boiling conditions can be related to three phenomena: deposition due to the bubble growth process (called boiling deposition), bubble induced concentration increase at crud-coolant interface (called enrichment and modelled by the enrichment factor, the ratio between the wall concentration and the bulk concentration) and vaporization induced concentration increase inside the crud. A literature review on the modelling of these phenomena and on the crud structure in nucleate boiling conditions has been carried out. The OSCAR [1] calculation code developed by CEA to predict surface and volume activities in a monophasic PWR primary circuit was chosen as a basis for present study. Ability to describe local nucleate boiling conditions was added to this code leading to realistic modelling of subsequent volume activity increase.

In this article, we present a new version of OSCAR calculation code including:

- A double phase thermal-hydraulic module,
- A model of boiling crud growth, able to calculate inner crud deposit physical parameters,
- A model of boiling deposition for ionic and particle species,
- A model of boiling precipitation in the crud,
- An adaptation of the precipitation model, which takes into account the enrichment factor.

With these new improvements, we are able to calculate the influence of local boiling in some cases. The mains first results are:

- A thicker deposit in boiling regions (ten times thicker than an non boiling deposit), thicker with higher thermal flux,
- Domination of boiling crud growth by enrichment enhanced precipitation in boiling region ,
- Some corrosion products behaviour can be changed by boiling. Indeed, iron is dissolved if its concentration is high enough at the wall in the hot part of fuel assembly, but in boiling conditions, calculations indicate precipitation of iron.

This contribution focuses on crud structure, crud growth phenomenology in nucleate boiling conditions, crud growth mechanism modelling in nucleate boiling conditions, selected thermal-hydraulic models for nucleate boiling parameters computation and initial results from the adapted version of the OSCAR code and their comparison to experimental feedback from PWRs.

Introduction

PWR primary circuit materials undergo general corrosion leading to a release of metallic elements. The main contributors are nickel and iron. Nickel comes from steam generators tubbing (Inconel 600 or Inconel 690) that correspond to about 70 % of the total surface of the primary circuit. Iron comes from stainless steel primary pipes corresponding to about 2 % of the total surface of the primary circuit.

The ^{58}Co volume activity in the primary circuit of a PWR is low and almost constant (< 30 MBq.m^{-3}) throughout an ordinary operating cycle. In some specific cases, a significant increase in volume activity is observed after the middle of a cycle (100-1000 MBq.m^{-3} for ^{58}Co) as shown in Figure 1. All isotopes do not have the same behaviour; for example the volume activity of ^{60}Co is almost constant.

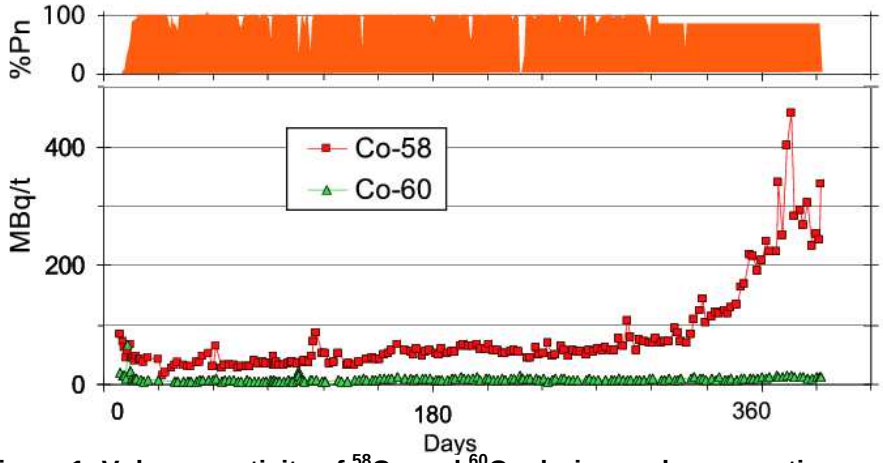

Figure 1: Volumes activity of ^{58}Co and ^{60}Co during and an operating cycle.

This significant increase in activity is attributed to nucleate boiling conditions. Boiling, indeed, is well known to increase the deposition/precipitation rates on heated surfaces, causing much higher crud thicknesses to be reached than in the case of no boiling. Boiling is also a key factor in the structure and the chemical characteristics of the crud.

Crud growth is governed by balance between the deposition/precipitation and the removal flux. If the deposited mass on fuel assembly cladding increases due to the boiling process, the mass of activated elements increases as well. Therefore, a larger amount of activated crud will be eroded and the total volume activity of the primary fluid will increase. The feedback experience shows that the volume activity is under particle form.

A threshold effect is also present in this balance between erosion and deposition/precipitation flux. Indeed, the volume activity increases at the end of the third cycle of a fuel assembly when crud thickness is large enough to involve a significant erosion flux. When it occurs, boiling is located in the hot part of fuel assemblies, in fuel assembly upper quarter region.

The modelling of these two fluxes (deposition/precipitation and erosion) and the modelling of boiling conditions are essential in providing a realistic calculation of these observed volume activity rises. In this article, we shall specifically focus on the effects of boiling on the deposition/precipitation term.

1. Crud structure

Without boiling process, the structure of corrosion product deposits on the cladding of the fuel rods seems more porous than the one on steam generator tubing (in the primary circuit). In the case of nucleate boiling, the crud is perforated by a regular arrangement of chimneys with an approximate 5 µm diameter growing perpendicular to the flow direction, as shown in Figure 2.

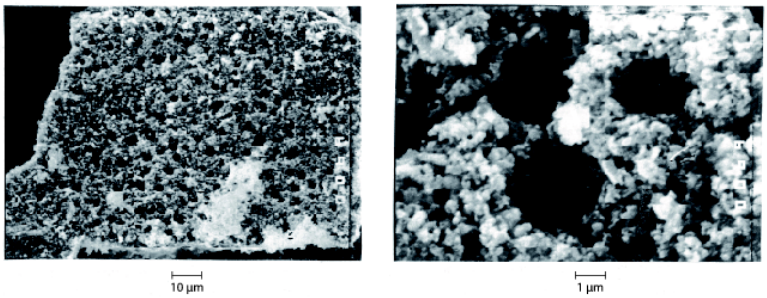

Figure 2: Global view (left) and detailed view (right) of porous structure of the crud observed in the CEA test loop facility CIRENE (in boiling conditions) [2].

According to Peybernès [2] and Billot [3] the conductivity of the crud is around 0.01 $W.cm^{-1}.K^{-1}$ and with a 100 $W.cm^{-2}$ thermal flux density, the temperature at the interface oxide/crud should increase by 1 °C per micrometer of crud. However, these temperature increases have never been observed. Macbeth [4] and Pan [5] show that the temperature gradient in the crud is significantly lower than in the case of pure conduction calculations (see Figure 3). This experimental result is a clear indication that part of the heat flux is removed by the wick boiling process through the chimneys. In this process, the part of the heat flux removed by evaporation becomes greater as the crud grows.

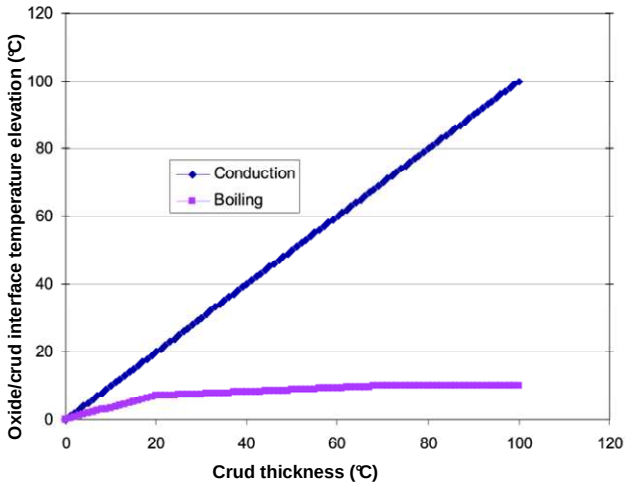

Figure 3: Temperature evolution at the oxide/crud interface [2].

The crud structure is described by Macbeth [4]:

- Chimney density: 5000 $ch.mm^{-2}$,
- Chimney diameter: 5 µm,
- Pore diameter: 0.1 to 0.5 µm,
- Average distance between two chimneys: 14 µm,
- Average voidage of the crud 70% with 10% due to chimneys.

We shall assume that all the fluid that flows through the pores towards the base of the chimneys is evaporated.

The precipitation process is also a key factor in the structure of boiling deposits. Indeed, precipitation could be considered as a “consolidating” process, in the way that the ionic species which precipitate in the pores of the crud consolidate the crud and fill the pores. In the case of boiling crud, the precipitation of ionic species occurs at the bottom of the chimneys, so only the deposit under this line will be consolidated.

According to studies of crud structure managed by EPRI [6] and with the assumption above we propose to adopt as structure of the crud what is shown in Figure 4:

- Superheated vapour layer,
- Crud/oxide layer which has an average porosity (~ 0.5),
- High porosity crud layer (~ 0.7).

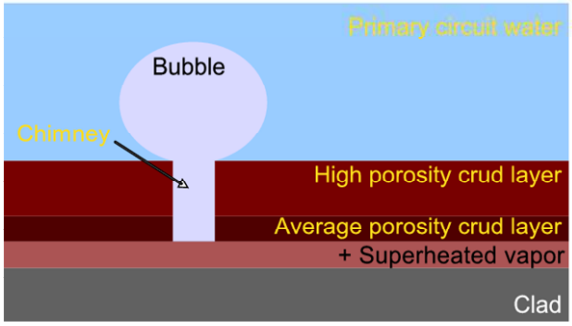

Figure 4: Crud structure description.

The modelling of the boiling crud greatly depends on the crud/fluid interface. We can consider three scenarios as a function of boiling conditions:

1. If the wall temperature (crud/fluid interface) is higher than the boiling temperature (T_{sat} + ΔT_{sat}), the new deposit will be a porous boiling deposit (~ 70% - 80% of voidage). As the crud grows, the porosity at the base of the deposit (oxide/crud interface) decreases because of the precipitation process. The crud is divided in two areas, the bottom one has some porosity and, the top one is more porous. The boiling temperature is lower in the case of a porous medium than in the case of a heated surface in contact with the fluid. Thus, as the crud grows, the boiling line moves from the crud/fluid interface to the oxide/crud interface. The vapour layer is slightly mixed with the average porosity crud layer, under the boiling line.
2. If the wall temperature is lower than the boiling temperature, there is no boiling at the wall. Until the boiling temperature is reached at the base of the crud, only monophasic deposition processes contribute to the crud growth. As the crud grows, the temperature at the oxide/crud interface increases, until the latter reaches boiling temperature. In this scenario we assume that the boiling line divides the crud in the two areas, cited previously. The link between the scenario with or without boiling is illustrated by Figure 5:
   a. Deposition and precipitation without boiling,
   b. Beginning of boiling, the temperature at the base of the crud is equal to the boiling temperature,
   c. Boiling is significant enough to create a vapour layer at the base of the deposit; the vapour is exhausted by chimneys.

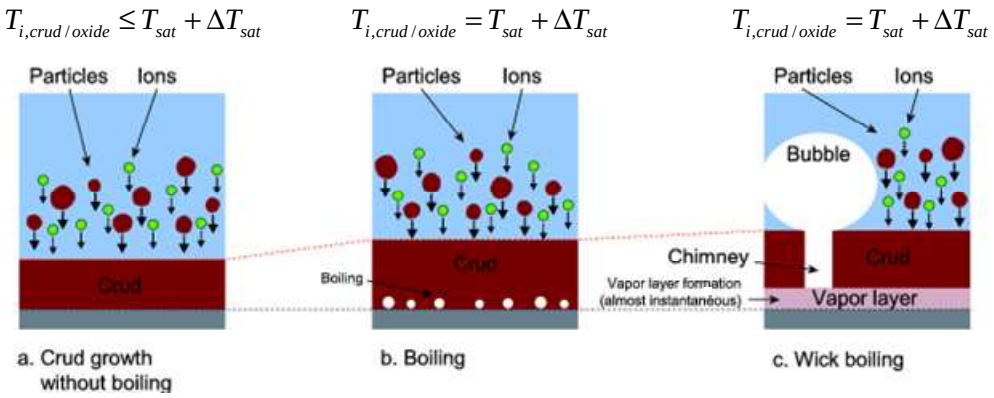

Figure 5: Illustration of three main steps from non-boiling to boiling conditions (with $T_{i,crud/oxide}$ the crud/oxide interface temperature and T_{sat} + ΔT_{sat} the boiling temperature).

3. If the wall temperature is much lower than the boiling temperature, the crud layer will only increase by deposition/precipitation mechanisms without boiling.

2. Deposition rate mechanism in boiling conditions

The deposition velocity can generally be subdivided in the case of the monophasic liquid flow in:

- Brownian deposition velocity,
- Turbulent deposition velocity,
- Inertial deposition velocity,
- Thermophoresis deposition velocity.

In the case of boiling flow, we have to add a new term of velocity, called “the boiling deposition velocity” due to the bubble formation at the heated surface.

The bubble formation process can be summarized in three steps illustrated in Figure 6 [7]:

1. Initial step (1): growing of a new bubble embryo on a nucleation site.
2. Intermediate step (1 → 2): the bubble grows quickly, mainly in the direction parallel to the flow rate. A micro-layer of fluid is stuck between the bubble and the heating surface.
3. For a relatively longer period of time the bubble grows rather vertically relative to the heating surface. This growth is caused by vaporization of the micro-layer of fluid. The vaporization of the micro-layer leads to the formation of a dry area at the base of the bubble on the heating surface. Once the critical diameter is reached, the bubble slides along the wall, where it can coalesce with other bubbles. After a series of coalescences, the bubble attains the diameter that will permit its ejection into the fluid.

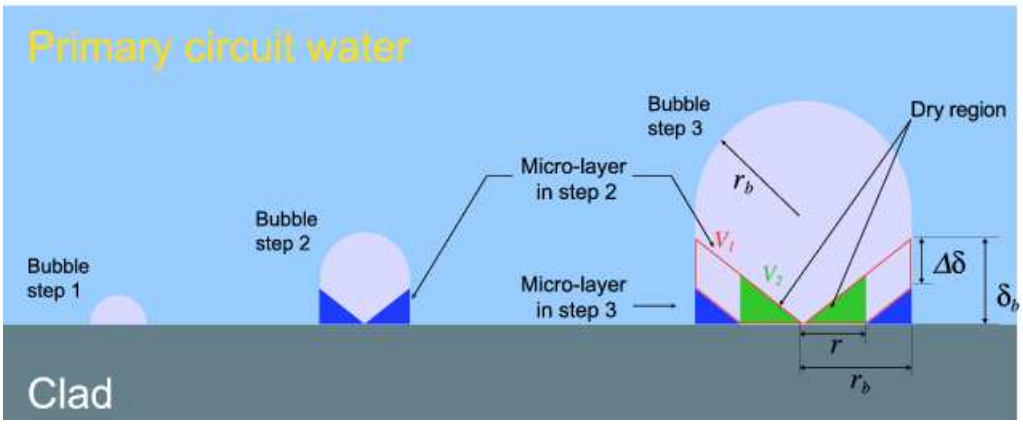

Figure 6: Formation of a bubble on a heated surface.

According to Asakura [8], the particles contained in the micro-layer of the fluid, micro-layer which is vaporised to create the dry region, are deposited on the wall. This is the nucleation of bubbles responsible for the boiling deposition.

The Asakura mechanism is schematized by the last step of Figure 6. Between stages 2 and 3, a dry contact region between the bubble and clad surface appears by the vaporization of the micro-layer volume V_1. Thus all particles initially contained in the V_2 volume are deposited on the heated surface. Micro-layer surrounding this dry surface prevents deposition of the other particles from V_1.
At the same time, the concentration of ionic species increases as the bubble grows (i.e. as the micro-layer is vaporised) until reaching the solubility limit. The ionic species in the V_2 volume thereby precipitate on the surface or on particles already on the wall. Corrosion products are not considered to be volatile.

The surface boiling deposition rate [8] can be expressed as:

$$\frac{dm}{dt} = K \cdot \frac{\phi}{L} \cdot C$$

With m the boiling deposited mass density (kg.m^{-2}), ϕ the surface heat flux (kg.m^{-2}.s^{-1}), L the latent heat (J.kg^{-1}), C the concentration of particles/ions in the fluid (kg.kg^{-1}) and K a constant.

According to Asakura, the K constant is the ratio between the V_2 volume (volume which contains the particles/ions that will be deposited on the surface) and the V_1 volume (the entire volume used to form the bubble between phases 2 and 3).

The K constant can be calculated by simple geometric assumptions [8]:
With the notations from Figure 6:

$$V_1 = \pi \cdot \Delta\delta \left({R_b}^2 - \frac{1}{3} r^2 \right)$$

$$V_2 = \frac{2}{3} \cdot \pi \cdot r^2 \cdot \Delta\delta$$

$$r = R_b \cdot \frac{\Delta\delta}{\delta_b}$$

If we assume that the entire vaporization of V_1 leads to a bubble with a maximum diameter (R_b the critical diameter) the expression of V_1 can be simplified, and:

$$V_1 = \frac{4}{3} \cdot \pi \cdot {R_b}^3 \cdot \left(\frac{\rho_v}{\rho_l} \right)$$

If we also assume that $(\Delta\delta) << (\delta_b)$, then we have:

$$\Delta\delta \approx \frac{4}{3} \cdot \frac{R_b \cdot \rho_v}{\rho_l}$$

With theses assumptions, we can calculate the V_2 volume, and therefore the K constant:

$$V_2 = \frac{2}{3} \cdot \pi \cdot \frac{{R_b}^2}{{\delta_b}^2} \cdot \left(\frac{4}{3} \right)^3 \cdot \frac{{R_b}^3 \cdot {\rho_v}^3}{{\rho_l}^3}$$

$$K = \frac{V_2}{V_1} = \frac{1}{2} \cdot \left(\frac{4}{3} \right)^3 \cdot \left(\frac{R_b}{\delta_b} \right)^2 \cdot \left(\frac{\rho_v}{\rho_l} \right)^2$$

Asakura uses $\frac{\phi}{L}$ for the vaporization rate with ϕ as heat flux density (W.m^{-2}) and L the latent heat of vaporisation. That means that the full heat flux is used for the vaporization. This assumption is valid only in the case of a saturated boiling, but not in the case of sub-saturated boiling as in PWR primary. We choose to replace to total heat flux by the evaporation heat flux ϕ_e in our model ($\dot{m}_v = \frac{\phi_e}{L}$). So, the expression of the surface boiling deposition rate is:

$$\frac{dm}{dt} = K \cdot \dot{m}_v \cdot C$$

In a PWR, the fluid sub-saturation is quite high (20 °C), bubbles are not necessarily ejected from the heated surface. “Equilibrium” bubbles are formed, which means that there is a balance between the evaporation and the condensation flux.

Boiling starts when the wall temperature (T_p) reaches the boiling temperature:

$$T_p \geq T_{sat} + \Delta T_{sat}$$

With T_{sat} the saturation temperature (°C) and ΔT_{sat} represent the overheating needed to have boiling (°C).

In the case of a porous media, the overheating needed to reach boiling conditions is lower than the overheating in the case of a surface in contact with the fluid. So, as the crud grows, the boiling temperature is reached deeper in the crud deposit as shown in Figure 3 (the position of the boiling line does not vary in the crud but the thickness does due to deposition/precipitation processes).

In the case of bubbles formed in the crud and not on the heated surface in contact with the fluid, the expression given by Asakura is not valid. Indeed, in this case, all the fluid coming from pores is used for the bubble formation. Thus, all particles and ions contained in the fluid are vaporised in order to form the bubble and feed the deposit. In this case, the constant K is equal to 1.
Thus, as the crud grows, boiling occurs deeper in the crud. And the K constant will vary between the value calculated by Asakura and one.

The micro-layer thickness calculation is essential in this model. The bubble growth is calculated by using the Unal modelling [9].

The micro-layer thickness is calculated by the Torigai expression [10]:

$${\delta_b}^2(R) = \frac{\mu \cdot U \cdot R^2}{2 \cdot \sigma + Pi \cdot R_b}$$

With, μ as the dynamic viscosity (kg.m^{-1}.s^{-1}), U the bubble growth velocity (m.s^{-1}), R the radius of bubbles (m), R_b the critical radius (m), σ superficial tension (J.m^{-2}) and Pi characterize the dynamic contribution due to the motion of the liquid surrounding the bubble.

Pi is calculated from the Rayleigh equation:

$$Pi = \rho_l \left(R \cdot \frac{dU}{dt} + \frac{3}{2} \cdot U^2 \right) + 4 \cdot \mu \cdot \frac{U}{R}$$

With ρ_l the fluid density (kg.m^{-3}).

3. Enrichment mechanism at the wall surface under boiling conditions

The bubble growth at the wall surface involves an imbalance between the in and out radial flow rates of fluid. This leads, in the liquid phase, to a concentration of particle and ionic species higher in the region of the fluid very close to the wall than in a case with no boiling.

We consider a fluid region divided as shown on Figure 7 [11],

- A layer that is not be disordered by the turbulences of the primary fluid (Zone L):
  We assume that the concentration of every considered species is practically constant in this region of fluid (C_p). The thickness of this layer amounts approximately to the one of the laminar layer.
- An intermediate layer (Zone P), where turbulences homogenize the fluid. Thus the concentration of each species tends to be equal to the bulk concentration. The thickness of this layer of fluid is assumed to be equal to the average critical radius of bubbles, so that the condensation flux of the bubble can be neglected.
- A fully turbulent layer (Zone C), where the concentration of each species is equal to the bulk concentration.

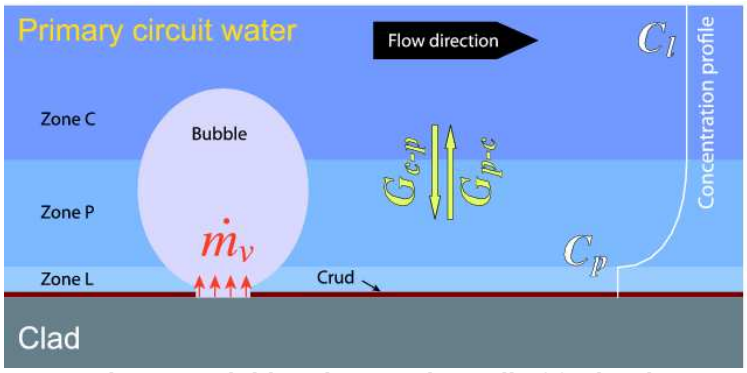

Figure 7: Fluid regions at the wall of fuel rod.

In order to explain this disequilibrium due to the boiling phenomenon, we calculate a mass balance in a section of fluid in the primary fluid (zone P + L):
The mass balance can be expressed as at z height:

$$\dot{m}_v \cdot C_v + G_{p-c} \cdot C_{p-c} = G_{c-p} \cdot C_{c-p}$$

With, $\dot{m}_v$ representing the vaporisation rate (kg.m^{-2}.s^{-1}), C_v the concentration of the species in the vapour phase (kg.m^{-3}), $G_{c\text{-}p}$ the fluid radial flow rate from zone C to zone P (kg.m^{-2}.s^{-1}), $C_{p\text{-}c}$ the concentration of the species in the zone P (kg.m^{-3}), $G_{p\text{-}c}$ the fluid radial flow rate from zone P to zone C (kg.m^{-2}.s^{-1}), $C_{c\text{-}p}$ the concentration of the species in zone C (kg.m^{-3}).

We can assume that:

- $C_{c-p} = C_l = \frac{1}{(1-x)+\Gamma \cdot x} \cdot C_0$, by considering that the concentration of the species in zone C is equal to the concentration of the species in the liquid phase.
- C_{p-c} varies in this way in zone P:

$$C_{p-c} = k \cdot C_P + (1-k) \cdot C_l$$

With, C_0 the bulk concentration at core inlet (kg.m^{-3}), x the mass quality, $\Gamma = \frac{C_v}{C_l}$ the repartition coefficient between vapour and liquid and k $(0 \le k \le 1)$ a constant depending of the thickness of zone P and the thickness of the layer near the wall where the concentration is constant.

The expression of the so-called enrichment factor, the ratio between the wall concentration and the bulk concentration of a considered species is given by:

$$F_E = \frac{C_p}{C_0} = \frac{n_c + (1/k)\cdot(1-\Gamma) - 1}{n_c} \cdot \frac{1}{(1-x) + \Gamma \cdot x}$$

With $n_c = \frac{G_{c-p}}{\dot{m}_v}$ the circulation number.

The concentration at the wall is higher under boiling conditions, implying a higher rate of precipitation. The precipitation mechanism can be expressed by:

$$\frac{dm}{dt} = \frac{1}{R}.\left(F_E.C_0 - C_{eq}\right)$$

With m the mass density which precipitates on the crud (kg.m^{-2}), R the transfer resistance (m.s^{-1}), F_E the enrichment factor, C_0 the bulk concentration (kg.m^{-3}) and C_{eq} the equilibrium concentration at the wall for the considerate specie.

In the previous section, we have seen that the deposition flux is proportional to the bulk concentration. However in boiling conditions, the concentration is higher near the wall than in the bulk. Thus, we propose to take into account the enrichment factor in the expression of the boiling deposition mechanism:

$$\frac{dm}{dt} = K \cdot \dot{m}_v \cdot F_E \cdot C_0$$

With, F_E as the enrichment factor, m the mass density deposited (kg.m^{-2}), $\dot{m}_v$ the vaporization rate (kg.m^{-2}.s^{-1}), C the particles/ions bulk concentration (kg.kg^{-1}), and K a constant.

Similarly, all mechanisms of deposition in simple phase must be impacted by this enrichment factor.

4. OSCAR calculations

The purpose of the OSCAR code [1], developed by the CEA in cooperation with EDF and AREVA NP, is to predict the contamination of the PWR primary system. The OSCAR code allows to simulate the behaviour of corrosion products, fission products and actinides and to calculate the volume activity in the fluid and the surface activity in the monophasic primary system. The OSCAR code is now considered to be a relevant tool both for numerical simulations or predictions and combining and organizing all knowledge useful to progress on contamination caused by activated corrosion products, fission products and actinides.

The code version used in the following calculations is a modified version of OSCAR V1.2 implemented with our boiling models.

We have performed three kinds of calculations with OSCAR in order to:

- Compare the deposition and the precipitation flux previously presented,
- Estimate the influence of boiling,
- Compare the results obtained from our model with literature (value of K) in the case of deposition.

4.1. Comparison between boiling precipitation and boiling deposition

As stated before, the crud growth is due to a double process of precipitation and deposition. Results of three calculations are displayed in figure 8:

- Without boiling mechanisms (single phase mechanisms only),
- With single phase mechanisms and boiling deposition mechanism without enrichment,
- With single phase mechanisms, boiling deposition and enrichment.

The calculation is divided in two periods:

- 65 days with no boiling process,
- 285 days with local boiling conditions.

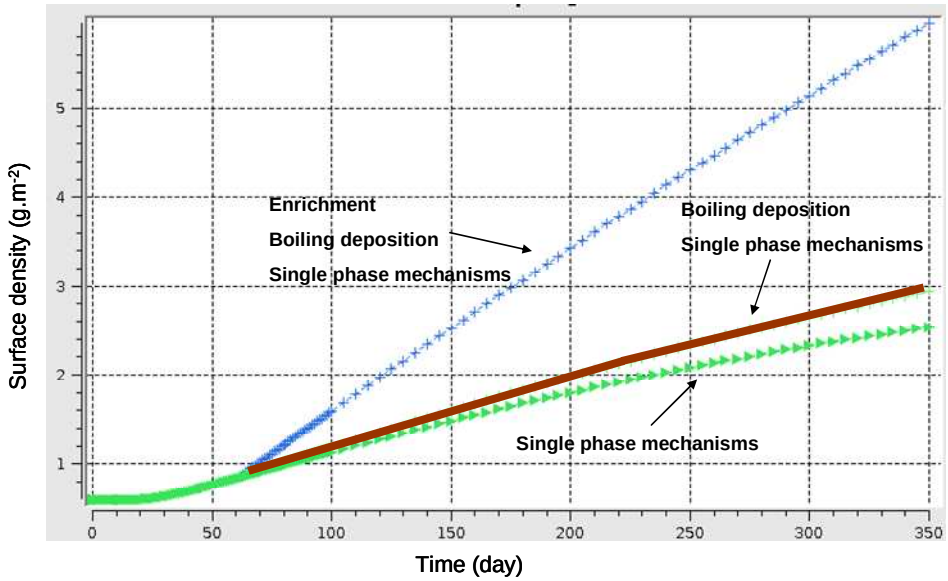

Figure 8: Comparison between boiling mechanisms (P = 155 bar, ϕ = 2.5 MW.m^{-2}, T_{cold} = 288.7 °C, T_{fluide} = 340 °C in boiling regions, no initial deposit, b oiling begins on the 65th day of calculation).

Figure 8 clearly shows that the precipitation flux enhanced by enrichment process leads to higher surface density than the boiling deposition flux.

4.2. Influence of boiling

We have performed a calculation with two different thermal density fluxes using the boiling models presented above, in conditions shown in Table 1. These calculations show the influence of boiling (i.e. the influence of the thermal density flux) on the total deposition and on some corrosion products like iron, nickel and chromium.

Parameters	Values	
Type of reactor	REP 1300 MW	
Pressure (bar)	155	
Core inlet (°C)	288.7	
Core outlet (°C) (average)	325	
Initial deposit mass density (g.m^{-2})	0.6	
	Calculation 1	Calculation 2
Thermal density flux (MW.m^{-2}) (boiling region)	1.0	2.0

Table 1 : Input parameters for calculations

Figure 9 displays evolution of the mass density deposited on a boiling surface, and on a non-boiling surface of fuel assemblies. In this calculation, boiling occurs on 1/3 of assemblies in the hot part of the fuel assemblies.
We can see that the mass density deposited is higher by a factor of up to 10 in local boiling conditions. The deposited mass also depends on the boiling conditions; indeed, in the case of the calculation with a thermal density flux of 2.0 MW.m^{-2} the mass density deposited is higher than in the case of the calculation with a thermal density flux of 1.0 MW.m^{-2}.

The calculation was carried out in the following conditions:

- 100 days with no boiling
- 250 days with boiling on the top of 1/3 of fuel assemblies

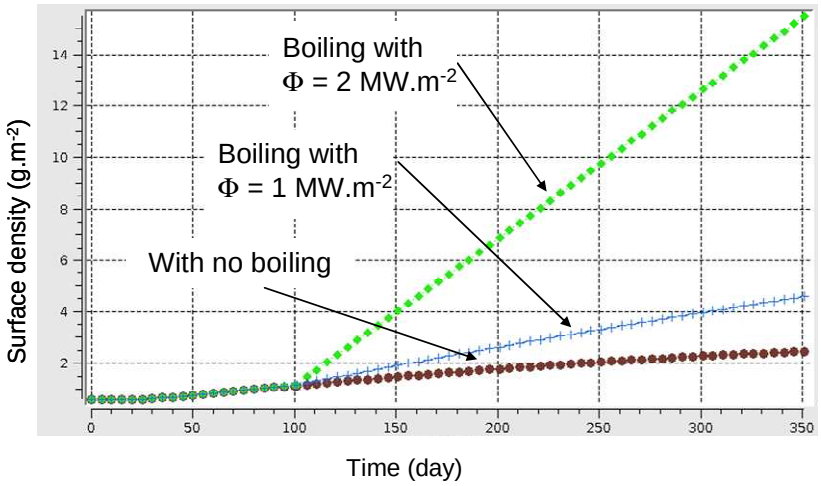

Figure 9: OSCAR calculation in boiling region (Boiling process starts on the 100th day).

The previous calculations are performed in the case of homogeneous deposits in the boiling region. The calculation of thickness depends on many parameters such as porosity, chemical phases, but we are able to estimate the maximum crud thickness (density[1] of the crud ~ 1 $g.cm^{-2}$):

- Boiling 1: ~ 4 µm,
- Boiling 2: ~ 15 µm,
- No boiling: ~ 3 µm.

In the following calculation the influence of boiling on some corrosion products is presented.

- Iron concentration

When there is no boiling, OSCAR assesses that the quantity of iron on the top of the assembly decreases progressively by dissolution and erosion. With boiling, it is the opposite; the enrichment factor is large enough to set the concentration of iron at the wall greater than the solubility, as shown in **Erreur ! Source du renvoi introuvable.**.

The temperature at the fluid/crud interface increases between the non boiling and the boiling phases.
The solubility of iron increases with the temperature (between 300°C and 345°C) and that is why, befor e the 150th day of the cycle iron is dissolved. After the 150th day, boiling precipitation and deposition are significant enough to reverse the tendency.
During the oxygenation phase, nickel crud is dissolved (especially at the top of the fuel assembly where the nickel concentration is the highest). Iron precipitation, in this part of the fuel, allows to have more stable oxides in relation to dissolution, which are not followed by a ^{58}Co volume activity peak during the oxygenation phase.

- Nickel and chromium concentrations

Nickel is the major component of the crud. The precipitation flux of nickel and chromium is also higher in boiling regions. The mass density of these elements in boiling regions follows the same tendency as the curves in Figure 9 (surface activity increases as soon as boiling starts).

[1] The density is calculated by using the density of the nickel ferrite (5330 $kg.m^{-3}$), a porosity of 0.8 and a stoichiometry of 0.3.

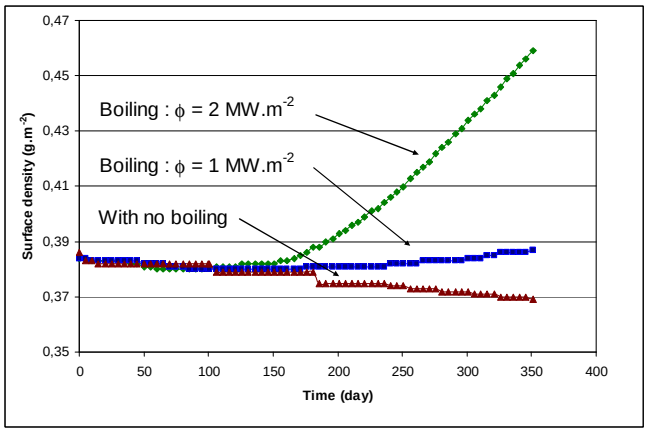

Figure 10: Iron precipitation in boiling regions (conditions of Table 1).

4.3. Comparison of the boiling deposition mechanism with literature

In the available literature, the boiling deposition mechanism has been widely studied and it seems that there is a consensus regarding the proportionality to the mass and heat flux. The differences between authors concern the value of the K proportionality constant. Some values of K are presented in Table 2.

Authors	Conditions	K
Beslu (CEA)	Primary conditions	0.84
Asakura [8]	Secondary conditions	0.29
Keefer et al. [12] Hu et al. [13]	Secondary conditions	0.29
Rassokhim [14]	100 atm pH alcalin	0.0556
AECL [15]	Secondary conditions	0.05

Table 2: Value of K.

The value of K, calculated by the presented model varies between 0.09 and 1 with the crud thickness.

In Figure 11, we have plotted the mass density with the different values of K, referenced in Table 2 and in the presented model. The calculation has been performed with a high particle concentration in the bulk and in primary conditions.

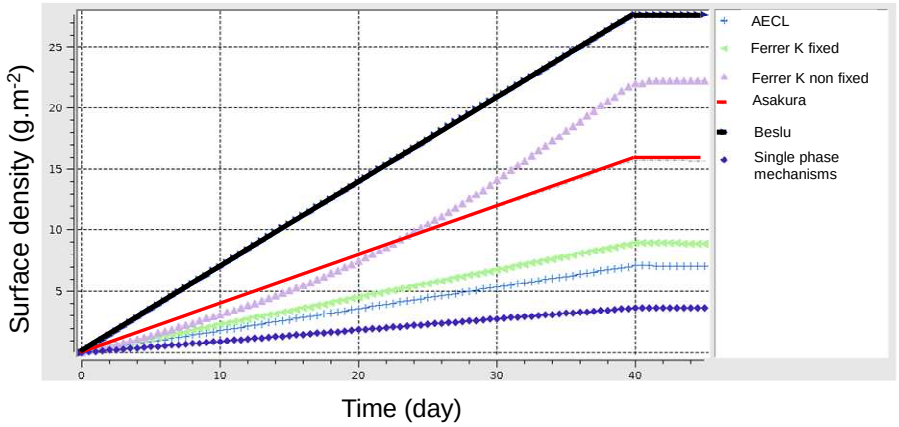

Figure 11: High particle concentration (143 bars, T_{cold} = 280 °C, 75.8 W.cm $^{-2}$, boiling stops at 40th day).

In the case of ''Ferrer K fixed'', the value of K is 0.09 and in the case of ''Ferrer K non-fixed'', the value of K varies from 0.09 to ~ 0.7.
As the crud grows, the temperature at the oxide/crud interface increases as does the vaporization rate (not model in Figure 11). Precipitation and deposition flux enhanced by enrichment are higher.
The boiling deposition process is greater when the K constant is close to 1.0 and F_E is around 1.2.

5. Conclusion

The literature review leads to consider two types of mechanisms to model crud growth under boiling conditions:

- an enrichment mechanism,
- a boiling deposition model.

Under boiling conditions, the enrichment factor is taken into account in the precipitation mechanism implying greater precipitation. A model of boiling deposition in primary PWR conditions has also been developed. Some improvements have been done in the calculation of the vaporisation rate and of the K constant (it now depends on crud thickness, and can vary between a value calculated at the surface of the crud and 1 in the case of crud inner boiling). This review leads to a new crud growth phenomenology, considering precipitation process in the crud due to inner boiling.

A new version of the OSCAR calculation code has been developed, including:

- A double phase thermal-hydraulic module,
- A model of boiling crud growth, able to calculate inner crud deposit physical parameters,
- A model of boiling deposition for ionic and particle species,
- A model of boiling precipitation in the crud,
- An adaptation of the precipitation model, which takes into account the enrichment factor.

When local boiling process occurs on the upper part of third-cycle fuel assemblies, calculations of crud growth show that the crud thickness can reach ten to a hundred times the thickness reached in pure single phase flow. This growth is mainly governed by the precipitation process enhanced by enrichment. However if we consider a K constant close to 1, the boiling deposition process becomes more significant.

The erosion flux also becomes greater when crud grows. Indeed, the fluid forces particularly the lifting and the drag forces, become higher and higher. As the crud grows, deposition and precipitation fluxes increase (K and vaporization rate increase) inducing a rise of oxide/crud interface temperature and a vaporization rate increase. Since this process happens in reactor neutron flux, the quantity of unwanted activated material becomes more and more significant and thus, the volume activity due to contamination of the primary fluid increases.

An experiment in the CIRENE [16] test loop at the CEA is foreseen in order to validate the particle boiling deposition model under primary conditions.

We expect that the new erosion model will be able to predict accurately these activity increases. Future work will also focus on the behaviour of each isotope during this process. Indeed, some measurements of activity in PWR plants show that the volume activity of ^{58}Co and ^{51}Cr grows significantly while the ^{60}Co volume activity does not increase. Speciation is also an essential parameter to consider; these increases in volume activity during an operating cycle are not followed by a volume activity peak during the oxygenation phase. That means, that boiling processes lead to the formation of “stable” oxides, which are not dissolved during the oxygenation phase.

References

[1] F. Dacquait, J. Francescatto, F. Broutin, J.B. Génin, G. Bénier, D. You, G. Ranchoux, J. Bonnefon, M. Bachet, G. Riot, ‘‘**Simulations of corrosion product transfer with the OSCAR V1.2 code**’’, this conference (2012)

[2] J. Peybernes, ‘‘**Influence de l’ébullition sur la corrosion externe des gaines de crayons combustibles des réacteurs à eau pressurisées**’’, PhD thesis, 1994

[3] P. Billot ‘‘**Etude du dépôt de produits de corrosion sur les éléments combustibles des réacteurs à eau pressurisé dans les conditions d’ébullition nucléée**’’, PhD thesis, 1983

[4] R.V. Macbeth, R. Tremberth, R. W. Wood, ‘‘**An investigation into the effect of crud deposits on surface temperature, dry-out and pressure drop, with forced convection boiling of water at 69 bar in an annular test section**’’, AEAW-R-705, 1971

[5] C. Pan, B. G. Jones, A. J. Machiels, ‘‘**Concentration level of solutes in porous deposits with chimneys under wick boiling conditions**’’, University of Illinois, EPRI, 1987

[6] Barclay G. Jones, ‘‘**Modelling and Thermal Performance Evaluation of Porous Crud Layers in Sub-Cooled Boiling Region of PWRs and Effects of Sub-Cooled Nucleate Boiling on Anomalous Porous Crud Deposition on the Fuel Pin Surface**’’, Department Nuclear, Plasma, and Radiological Engineering University of Illinois, 2005

[7] Van P. Carey, ‘‘**Liquid-Vapor Phase-Change Phenomena: an Introduction to the Thermophysics of Vaporization and Condensation Process in Heat Transfer Equipment**’’, 1984

[8] Y. Asakura, ‘‘**Deposit of Iron Oxide on Heated Surfaces in Boiling Water**’’, Hitachi Ltd., 1978

[9] H.C. Unal, ‘‘**Maximum bubble diameter, maximum bubble-growth time and bubble-growth rate during the subcooled nucleate flow boiling of water up to 17.7 MN/m²**’’, Int. J. Heat Mass Transfer, 1976

[10] K. Torigai, Trans JSME 1966; volume 32, pages 1263–1275

[11] P. March, ‘‘**Caractérisation et modélisation de l’environnement thermodynamique et chimique des gaines de combustible des réacteurs à eau sous pression en présence d’ébullition’’**, thèse, Université de Provence, 1999

[12] R. H. Keefer, J. L. Rider, L. A. Waldman, ‘‘**An Analytical Model for particulate Deposition on Vertical Heat Transfer Surfaces in Boiling Environment**’’, Bettis Atomic power Laboratory Westinghouse Electric Corporation, Conf 930627-1

[13] M. H. Hu, ‘‘**A Model for Sludge Distribution within Steam Generator**’’, Westinghouse Electric Corporation, NSD-JLH-5416

[14] N. G. Rassokhim et al., ‘‘**Iron Oxide Deposits on Heat Surfaces and their Removal in High Temperature High Pressure Electrochemistry in Aqueous Solutions**’’, p 245, R. W. Staehle and D. de G. Jones, Eds., National Association of Corrosion Engineers, Houston, 1976

[15] C.W. Turner, Y. Liner, M.B. Carver, ‘‘**Modelling Magnetite Particle Deposition in Nuclear Steam Generators and Comparison with Plant Data**’’, AECL-11128, COG-94-327

[16] M. Girard, R. Mombellet, G. Ranchoux, G. Riot, ‘‘**Experimental study of particle deposition kinetics in the primary circuit of the CIRENE loop and comparison with the OSCAR code simulations’’,** this conference (2012)